



Green tea extract improves cyclophosphamide-induced immunosuppression in mouse spleen and enhances the immune activity of RAW 264.7 cells

Jeong-Won Kim, Jin-Hwa Kim, Chang-Yeop Kim, Ji-Soo Jeong, Je-Won Ko^{*},
Tae-Won Kim^{**}

College of Veterinary Medicine (BK21 FOUR Program), Chungnam National University, 99 Daehak-ro, Daejeon, 34131, Republic of Korea

ARTICLE INFO

Keywords:

Green tea extract
Cyclophosphamide
Immunosuppression
Macrophage
Mitogen-activated protein kinases
Nuclear factor kappa B

ABSTRACT

Cyclophosphamide (CP) is mainly used to treat autoimmune diseases and cancer; however, it damages normal immune cells. Therefore, the effects of chemotherapy on CP are limited. Notably, green tea has been reported to effectively modulate immune function. Here, given the pharmacological properties of green tea, we evaluated the ability of green tea extract (GTE) to restore immunity suppressed by CP *in vivo* and to activate macrophages *in vitro*. GTE significantly improved the suppressed immune function, including spleen index and proliferation of spleen T lymphocytes, as revealed by histopathological examination and flow cytometry analysis. Moreover, GTE effectively activated RAW 264.7, as represented by the induction of nitric oxide, reactive oxygen species, and cytokine levels. GTE also increased the phosphorylation of mitogen-activated protein kinases (MAPKs) and nuclear factor kappa B in RAW 264.7 cells. In conclusion, GTE ameliorated CP-induced immunosuppression in mice and stimulated immune activity in RAW 264.7 cells, possibly by activating the MAPK signaling pathway. These findings suggest that GTE has the potential to be used as a supplementary agent in chemotherapy for CP.

1. Introduction

Cyclophosphamide (CP), a chemotherapy drug that suppresses the immune system, is mainly used to treat autoimmune diseases and cancer [1,2]. CP is a cytotoxic drug that causes cell death by damaging DNA structure and blocking its replication [3]; furthermore, its use in clinical chemotherapy is limited because it causes unintended immunosuppression, myelosuppression, and leukopenia by damaging normal immune cells [4–6].

The immunosuppressive effects of CP have undergone comprehensive investigation [7]. CP disrupts immune homeostasis by diminishing the regulatory T cell count, thus exerting its effectiveness [7]. In animal models, CP consistently induces regulatory T cell production through heightened apoptosis and disturbances in homeostasis, leading to alterations in the balance of lymphocyte subpopulations. Combination therapies employing multiple drugs alongside CP have been employed to enhance its efficacy and alleviate

^{*} Corresponding author College of Veterinary Medicine (BK21 FOUR Program), Chungnam National University, 99 Daehak-ro, Daejeon, 34131, Republic of Korea.

^{**} Corresponding author. College of Veterinary Medicine (BK21 FOUR Program), Chungnam National University, 99 Daehak-ro, Daejeon, 34131, Republic of Korea.

E-mail addresses: rheoda@cnu.ac.kr (J.-W. Ko), taewonkim@cnu.ac.kr (T.-W. Kim).

<https://doi.org/10.1016/j.heliyon.2023.e22062>

Received 5 April 2023; Received in revised form 11 September 2023; Accepted 31 October 2023

Available online 8 November 2023

2405-8440/© 2023 The Authors. Published by Elsevier Ltd. This is an open access article under the CC BY-NC-ND license (<http://creativecommons.org/licenses/by-nc-nd/4.0/>).

adverse effects; however, these approaches face limitations [8,9]. Furthermore, there remains a lack of safe and effective drugs for counteracting immunosuppression and other detrimental effects. Thus, the exploration of natural products holds promise in addressing these limitations. *Camellia sinensis* (green tea) is a natural plant with antioxidant properties [10] that contains catechins such as epicatechin (EC), epigallocatechin (EGC), EGC gallate (EGCG), gallic catechin gallate, and EC gallate (ECG) [11]. Catechins contained in green tea have been demonstrated to have antioxidant, anticancer, and antimicrobial properties [12–14]. Furthermore, green tea polyphenols, particularly EGCG and ECG, can significantly enhance immune responses and lower the risk of immune-related diseases [14,15]. Specifically, EGCG acts as an immunomodulator by regulating T-lymphocyte activity [16] and increases CD4⁺ and CD8⁺ lymphocyte counts, inducing Th1 responses. Furthermore, EGCG has conclusive effects on the growth of lymphoid cells and the immune system. Recent studies have shown that EGCG benefits autoimmunity by influencing the differentiation of naïve helper T cells into different effector subsets [17]; moreover, it specifically regulates CD4⁺ T-cell differentiation into Th9 cells and affects many types of immune cells in the innate and adaptive immune systems. Interestingly, research using autoimmune disease models has shown improved symptoms in animals administered with EGCG [18]. Despite these findings, mechanistic studies on GTE in CP-induced immunosuppression models are lacking. Based on these results, we hypothesized that green tea extract (GTE) exerts immunomodulatory effects against CP.

In this study, we examined the immune-enhancing effects of GTE on CP-induced immunosuppression by assessing the proliferation of immune cells and performing a histological analysis of the spleen. Furthermore, we evaluated GTE-induced macrophage activation by focusing on the activated mitogen-activated protein kinase (MAPKs) and nuclear factor kappa B (NF- κ B) signaling pathways in RAW 264.7 cells.

2. Materials and methods

2.1. GTE preparation

GTE was prepared as previously described [11]. The green tea leaves were purchased from Dajayeon (Seoul, South Korea). The leaves were then dried and ground into a powder. After sieving through a 50 mm mesh, the powder was dissolved in 70 % ethanol (1:10, v/v), and the upper layer was collected; this process was repeated in triplicate. The extract was freeze-dried (30 % extraction yield), and GTE contained 7 % EGC (catalog no. E3768; Sigma-Aldrich), 36 % catechin (Catalog no. 89172; Sigma-Aldrich), and 22 % EGCG (Catalog no. E4143; Sigma-Aldrich), as confirmed by high-performance liquid chromatography-ultraviolet analysis.

2.2. In vivo experiments

2.2.1. Animals and guidelines

Six-week-old male BALB/c mice (body weight, 19–21 g) were supplied by Orient Bio (Gyeonggi-do, Republic of Korea). Mice were provided ad libitum with water and pellet feed (Catalog no. 5053; Orient Bio) containing 21.0 % protein, 11.3 % fat, 4.4 % fiber, 56.3 % carbohydrates, 6.0 % minerals, and 1.0 % vitamins. After a one-week acclimatization period, the mice were randomly divided into four groups (n = 6 per group): NC (normal control; saline treatment), CP (CP treatment), GTE100 (CP treatment + GTE 100 mg/kg, per os [p.o.]), and GTE500 (CP treatment + GTE 500 mg/kg, p.o.). Notably, our research team confirmed GTE's safety in a preliminary study, with dose ranges for the animal studies at 100–500 mg/kg. In the dose-range-finding study, toxicity was not observed in the "GTE-only" control group. Importantly, GTE was dissolved in distilled water and orally administered daily for seven days. Moreover, NC and CP control mice were administered equal volumes of distilled water; CP (Catalog no. PHR1404; Sigma-Aldrich) was dissolved in saline solution, and the CP group was intraperitoneally injected with 100 mg/kg CP for two days, while the NC group was injected with equal volumes of saline. All mice were sacrificed 24 h after the last treatment with carbon dioxide, and the spleen tissue was harvested for fluorescence-activated cell sorting (FACS) and histopathological analysis. The animal experimental protocol was approved by the Institutional Animal Care and Use Committee of the Chungnam National University (202112A-CNU-191).

2.2.2. Body weight and spleen index

The mice were weighed using a digital scale to measure the body and spleen weights. Body weights were recorded from days 0–7. The spleens were harvested immediately and weighed at the end of the experiment. The spleen index (%) was calculated using the following formula:

$$\text{Spleen index (\%)} = \text{spleen weight (mg)} / \text{body weight (g)}.$$

2.2.3. Measurement of immune cells in the spleen

Single-cell suspensions were prepared from the spleen samples for visual confirmation of immune cell differentiation. Splenocytes were attached to glass slides using a cytospin device (Hanil Science Industrial, Seoul, Republic of Korea), dried, fixed, and stained using Diff-Quik® staining reagent (catalog no. 38721; Sysmex Corporation, Kobe, Japan). The slides were examined manually under a microscope (Leica DM LB2; Leica, Wetzlar, Germany). All the slides were assessed twice under an optical microscope in a blinded manner. Ten consecutive nonoverlapping fields were obtained per slide.

2.2.4. Flow cytometry

The spleen was harvested and processed into single cells. After passing the cell suspension through a 70 μ m cell strainer, the cells were washed with Dulbecco's modified Eagle's medium (DMEM; SH30243.01; HyClone, Incheon, Republic of Korea). Red blood cells

(RBC) were lysed in a lysis buffer (catalog no. 555899; BD Biosciences, San Jose, CA, USA). Cell viability was measured using trypan blue (15250061; Gibco, Grand Island, NY, USA). Cell suspensions were diluted to 1×10^6 cells/mL for analysis. To isolate different lymphocyte subsets, cells were stained with FITC Rat Anti-Mouse CD3 antibody (1:100 dilution; Catalog no. 561798; BD Biosciences) and PerCP Rat Anti-Mouse CD4 antibody (1:100 dilution; Catalog no. 553052; BD Biosciences) for 30 min at 4 °C in the dark. After washing the cells twice, FACS data were acquired and analyzed using a BD Accuri C6 Plus flow cytometer (BD Biosciences).

2.2.5. Histopathological examination

A portion of formalin-fixed spleen was processed, embedded in paraffin, and cut into 4 μ m thick sections. Sections were deparaffinized, rehydrated using standard techniques, stained with Harris hematoxylin and eosin (TissuePro Technology, Gainesville, FL, USA), and examined under a microscope (Leica DM LB2). All microscopic fields were randomly selected and observed manually under a light microscope using 10 \times and 20 \times objective lenses and a 100 \times oil immersion lens. Histological evaluation was performed by focusing on the clarity of the boundaries between the white and red pulps of the spleen.

2.3. In vitro experiments

2.3.1. Cell viability assay

The murine macrophage cell line, RAW 264.7, was maintained in DMEM supplemented with 10 % heat-inactivated fetal bovine serum, 100 U/mL penicillin, and 100 g/mL streptomycin at 37 °C in a humidified 5 % CO₂ incubator. RAW 264.7 cells were seeded at a 5×10^4 cells/well density in a 96-well plate. The plate was incubated overnight, and the cells were treated with various concentrations of GTE for 24 h ($n = 3$). Cell viability in response to GTE treatment was measured using the EZ-Cytox Cell Viability Assay Kit (DoGenBio Co., Ltd., Seoul, Republic of Korea). Briefly, after culturing for 24 h, 10 μ L of the kit solution was added to each well and incubated for 2 h at 37 °C under 5 % CO₂. Absorbance was measured at 450 nm using an enzyme-linked immunosorbent assay (ELISA) reader (Bio-Rad Laboratories, Hercules, CA, USA). The viability of the treated cells was determined relative to that of untreated control cells.

2.3.2. Analysis of nitric oxide (NO) production

RAW 264.7 cells (5×10^4 cells/well) were incubated with 20, 40, 80, and 160 μ g/mL of GTE and 0.5, 1 μ g/mL of lipopolysaccharide (LPS) for 24 h ($n = 3$). After incubation, the supernatants were collected and reacted with Griess reagent (Catalog No. ab65328; Abcam) according to the manufacturer's instructions. A NO₂ standard curve was used to calculate the nitrate concentration. The absorbance was measured at 450 nm using an ELISA plate reader (Bio-Rad Laboratories).

2.3.3. Analysis of reactive oxygen species (ROS) production

RAW 264.7 cells (5×10^4 cells/well) were incubated with 20, 40, 80, and 160 μ g/mL of GTE and 0.5, 1 μ g/mL of LPS for 24 h ($n = 3$). ROS formation in RAW 264.7 cells was detected using 2',7'-dichlorofluorescein (DCFDA), a cell-permeable reagent, which ROS oxidizes to form a fluorescent compound, with excitation and emission spectra of 495 and 529 nm, respectively; this experiment was performed using the DCFDA reagent (Catalog no. ab113851; Abcam), according to the manufacturer's instructions. Fluorescence was measured using a fluorescence plate reader (PerkinElmer).

2.3.4. Analysis of cytokine production

RAW 264.7 cells were incubated with 20, 40, 80, or 160 μ g/mL GTE and 1 μ g/mL LPS for 24 h ($n = 3$). The production of interleukin (IL)-6 and tumor necrosis factor (TNF)- α was assessed using a commercial ELISA kit (Catalog no. ELM-IL6-1, ELM-TNF α -1; Raybiotech, GA). Briefly, cell supernatants were collected from RAW 264.7 cell culture and centrifuged at 1200 \times g for 10 min to remove cell debris. Supernatants were processed according to the manufacturer's instructions. The samples were added to the coated plates and incubated for 2 h at room temperature. The plates were then incubated with biotin-conjugated antibodies for 1 h. After washing thrice, horseradish peroxidase-conjugated streptavidin was added to bind biotin, catalyzed by a tetramethylbenzidine reagent. The reaction was stopped by adding a stop solution, and the absorbance was measured at 450 nm using an ELISA plate reader (Bio-Rad Laboratories).

2.3.5. Analysis of mRNA expression levels

RAW 264.7 cells were incubated with 20, 40, 80, or 160 μ g/mL GTE and 1 μ g/mL LPS for 24 h ($n = 3$). The mRNA expression levels of IL-6 and TNF- α were determined as in a previous study [18]. Briefly, total RNA was isolated, and cDNA was synthesized using the SmartGene Total RNA Extraction Kit (SJ Bioscience, Daejeon, Republic of Korea) and Compact cDNA Synthesis Kit (SJ Bioscience) according to the manufacturer's protocol. SYBR Green-based quantitative polymerase chain reaction (qPCR) was performed using the CFX™ Connect Real-Time System (Bio-Rad Laboratories). The set of primers used for amplification were as follows: IL-6, forward, 5'-ATG CAA TAA CCA CCC CTG AC-3,' and reverse, 5'-ATC TGA GGT GCC CAT GCT AC-3'; TNF- α , forward, 5'-CAA AGT AGA CCT GCC CAG AC-3,' and reverse, 5'-GAC CTC TCT CTA ATC AGC CC-3'; and GAPDH, forward, 5'-GAT TTG GTC GTA TTG GGC GC-3,' and reverse, 5'-AGT GAT GGC ATG GAC TGT GG-3.'

2.3.6. Immunoblotting

The cells were treated with 40, 80, and 160 μ g/mL GTE and 0.5, 1 μ g/mL LPS for 24 h ($n = 3$). The cells were collected by washing twice with phosphate-buffered saline and resuspended in RIPA buffer (Sigma-Aldrich) containing a protease/phosphatase inhibitor (Sigma-Aldrich). Immunoblotting was performed as previously described [19,20]. Antibodies against the following proteins

(purchased from Abcam) were used: total extracellular signal-regulated kinase 1/2 (t-ERK1/2; 1:1000), phospho-ERK1/2 (p-ERK1/2; 1:1000), total c-Jun N-terminal kinase (JNK; 1:1000), p-JNK (1:1000), p38 (1:1000), p-p38 (1:1000), cytoplasmic p65 (1:1000), nuclear p65 (1:1000), α -tubulin (1:1000), lamin B1 (1:1000), laminin receptor (LR, 1:1000), and β -actin (1:2000). Relative protein expression was determined using a ChemiDoc (Bio-Rad Laboratories).

2.4. Statistical analyses

The results are expressed as mean \pm standard deviation (SD), and all statistical comparisons were determined using one-way analysis of variance (ANOVA) followed by post-hoc Tukey's Honestly Significant Difference test. Statistical significance between the treatment and NC groups was determined using GraphPad InStat v. 3.0 (GraphPad Software, Inc., La Jolla, CA). Statistical significance was set at a p value less than 0.05 or 0.01.

3. Results

3.1. In vivo experiments

3.1.1. Effects of GTE on spleen index in mice

Fig. 1 shows the spleen size and index of CP-induced mice treated with or without GTE. Analyses were performed on the day of sacrifice. Compared with the spleen size and index of the NC group, the CP group showed a marked reduction in these metrics ($p < 0.01$). The CP + GTE500 group (2.1 ± 0.32) showed an increased spleen index compared to that of the CP group (1.5 ± 0.30 , $p < 0.01$). Although the CP + GTE100 group (1.7 ± 0.16) did not show a significant spleen index value, a dose-dependent correlation was observed between the two groups. However, no significant differences in body weight were observed between groups (data not shown).

3.1.2. Effect of GTE on T lymphocytes subsets of the spleen

As shown in Fig. 2A, the lymphocyte population was markedly decreased in the CP group and was effectively restored in the CP + GTE group (indicated by red arrows). The results of differentiation of these T lymphocyte subsets are presented in Fig. 2B. Compared to those in the NC group (19.8 ± 2.81 %), the percentages of CD3⁺ and CD4⁺ T cells in the CP group (9.3 ± 0.29 %) decreased significantly ($p < 0.01$), indicating that an immunosuppressed mouse model was successfully constructed. Compared to those in the CP group (9.3 ± 0.29 %), the percentages of CD3⁺CD4⁺ T cells in the CP+GTE500 group (12.9 ± 0.40 %) increased significantly ($p < 0.01$); in particular, the CD3⁺/CD4⁺ ratio in the CP+GTE500 group (0.75) reached the same level as that observed in the NC group (0.75).

3.1.3. Effect of GTE on histopathology of the spleen

The NC group showed clearly differentiated T cell areas surrounding the central veins and clear lymphoid follicles, with a clear marginal zone of white pulp (dotted circle) and a clear boundary between the white and red pulp (Fig. 3). However, the CP group showed irregular and unclear differentiation of the spleen tissue compartments and indistinct and smaller lymphoid follicles than the NC group. These irregularities and visual ambiguities in the spleen compartments were largely restored in the CP + GTE group, especially in the CP + GTE500 group.

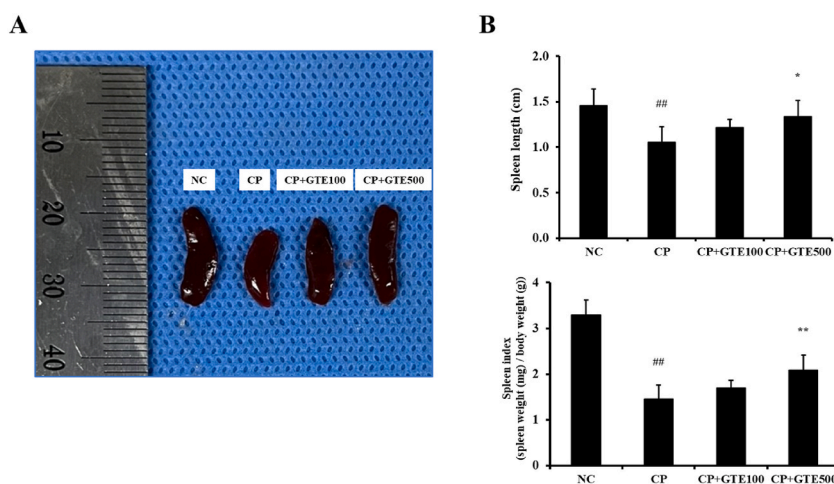


Fig. 1. Impact of green tea extract (GTE) on immune organ indices in immunosuppressed mice. (A) Representative spleen images and (B) spleen index. Mean values \pm SD ($n = 6$). # $p < 0.01$ vs. normal control (NC) group, * $p < 0.01$ vs. cyclophosphamide (CP) group. Bar = 10 mm.

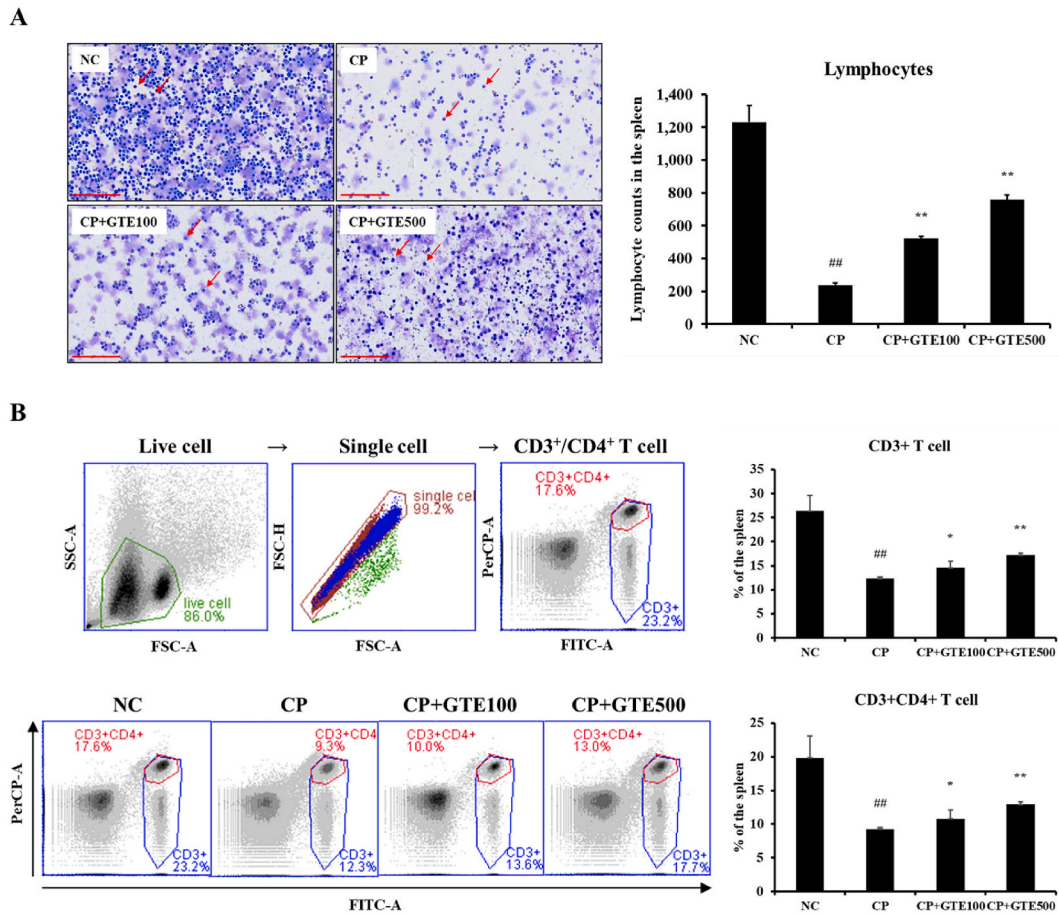


Fig. 2. Influence of green tea extract (GTE) on lymphocyte population and T lymphocyte subsets differentiation. (A) Lymphocyte population in the spleen shown through Diff-Quik® staining with cytopsin device, and (B) T lymphocyte subsets detected via flow cytometry. Mean values ± SD (n = 6). ^{##}p < 0.01 vs. NC group; ^{*}, ^{**}p < 0.05 and 0.01, respectively, vs. CP group. Bar = 100 μm.

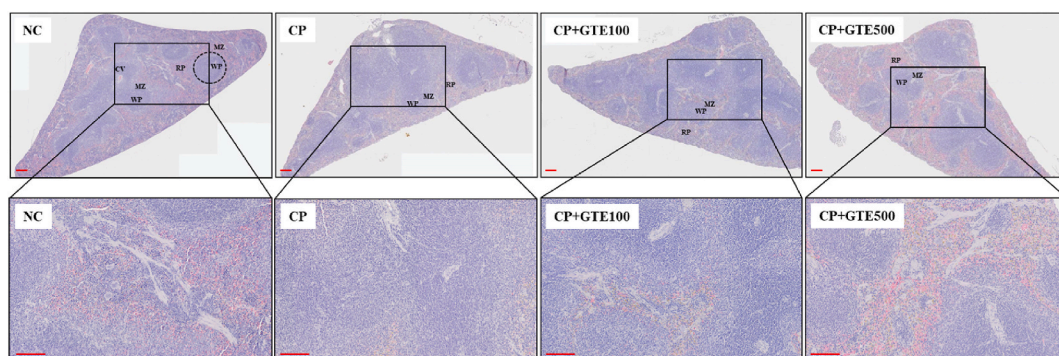


Fig. 3. Impact of green tea extract (GTE) on spleen histopathology. Normal control (NC) group received saline only; cyclophosphamide (CP) group treated with CP and saline; CP + GTE100 group treated with CP and GTE 100 mg/kg; CP + GTE500 group treated with CP and GTE 500 mg/kg. Histological images of spleen’s white pulp (WP), red pulp (RP), marginal zone (MZ), and central vein (CV). Bar = 100 μm.

3.2. In vitro experiments

3.2.1. Effect of GTE on cell viability, NO, and ROS production in RAW 264.7 cells

GTE did not have a cytotoxic effect on RAW 264.7 at concentrations up to 160 μg/mL for 24 h (Fig. 4A). Therefore, we used GTE concentrations up to 160 μg/mL for subsequent experiments. To examine whether GTE modulates immune activity, NO and ROS

production were measured in GTE-treated RAW 264.7 cells. As illustrated in Fig. 4B, the application of GTE led to a concentration-dependent elevation in NO production. Notably, GTE at 40 $\mu\text{g/mL}$ ($10.8 \pm 0.79 \mu\text{M}$) exhibited statistical significance ($p < 0.05$). Similarly, the fluorescence intensity representing ROS production in GTE-treated cells increased in a concentration-dependent manner, especially in the case of 80 $\mu\text{g/mL}$ of GTE (2.9 ± 0.57 , $p < 0.05$).

3.2.2. Effect of GTE on cytokines production in GTE-treated RAW 264.7 cells

To investigate the effects of GTE on immune modulation, the expression levels of IL-6 and TNF- α expression were examined in RAW 264.7 cells. As indicated in Fig. 5A and B, the qPCR results highlighted a trend of increasing mRNA levels for IL-6 and TNF- α in RAW 264.7 cells treated with GTE, with particularly noteworthy changes seen in the 80 and 160 $\mu\text{g/mL}$ GTE-treated groups ($p < 0.01$) compared to the changes in the control group. These results are consistent with the ELISA results that estimated the production of IL-6 and TNF- α in cell supernatants (Fig. 5C and D). IL-6 and TNF- α levels were markedly increased in GTE-treated cells and were statistically significant in the 160 $\mu\text{g/mL}$ GTE group ($p < 0.01$).

3.2.3. Effects of GTE on the MAPK pathway in RAW 264.7 cells

To analyze the mechanism by which GTE regulates immune responses, RAW 264.7 cells were grown in the presence of varying concentrations of GTE. GTE-treated cells exhibited a higher, concentration-dependent phosphorylation of MAPKs, including ERK, JNK, and p38, than did untreated cells (Fig. 6A). The phosphorylation of JNK in the group treated with 160 $\mu\text{g/mL}$ GTE was statistically significant ($p < 0.05$), while that of ERK and p38 was statistically significant in the groups treated with 80 and 160 $\mu\text{g/mL}$ GTE ($p < 0.05$). Translocation of NF- κB (p65) from the cytoplasm to the nucleus of cells showed results similar to those observed for ERK/JNK/p38 phosphorylation, and statistical significance was observed at a dose of over 40 $\mu\text{g/mL}$ GTE (Fig. 6B). Moreover, LR protein expression was increased significantly in the groups treated with 80 $\mu\text{g/mL}$ (1.7 ± 0.13 , $p < 0.05$) and 160 $\mu\text{g/mL}$ GTE (2.2 ± 0.05 , $p < 0.01$).

4. Discussion

CP, a chemotherapeutic drug, has notable immunosuppressive side effects that lead to the inhibition or killing of immune effector cells. Studies have shown that chemotherapy can affect lymphocytopenia, T cell inhibition, and natural killer (NK) cell proliferation [21]. Therefore, drugs that complement the immunosuppressive effects of CP need to be identified. Unlike chemical drugs, natural products have the advantage of being used as traditional medicines with fewer side effects and easy accessibility [22]. Heredy, we examined the immune enhancement by GTE against CP-induced immunosuppression in mouse spleens and studied its mechanism *in vitro*.

Lymphocytes, including natural killer (NK), T, and B cells, are white blood cell subtypes in the immune system. T cells are further divided into helper T (Th), memory T, or NK T cells [23]. Th cells are key regulators of the adaptive immune system [24]. Because the spleen is the main organ of T lymphocyte differentiation and the immunosuppressive effect of CP is represented by the inhibition of T lymphocyte differentiation and killing of immune cells, the spleen index and T lymphocyte count are used to evaluate immune capacity

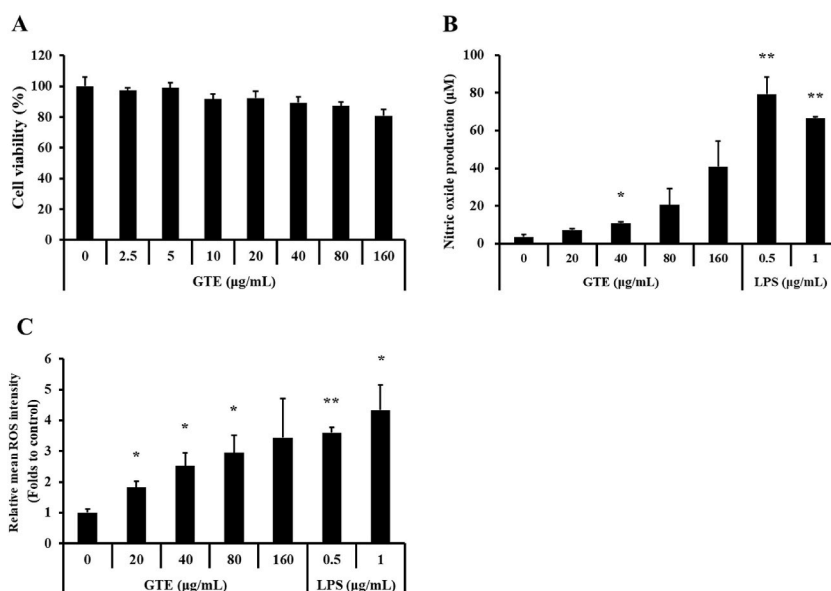


Fig. 4. Effect of green tea extract (GTE) on RAW 264.7 cell viability and nitric oxide (NO) and reactive oxygen species (ROS) production. (A) Impact of various GTE concentrations on RAW 264.7 cell viability, (B) NO production, and (C) ROS production. Lipopolysaccharide (LPS) used as positive control. Mean values \pm SD ($n = 3$). *, ** $p < 0.05$ and 0.01 , respectively, vs. NC group.

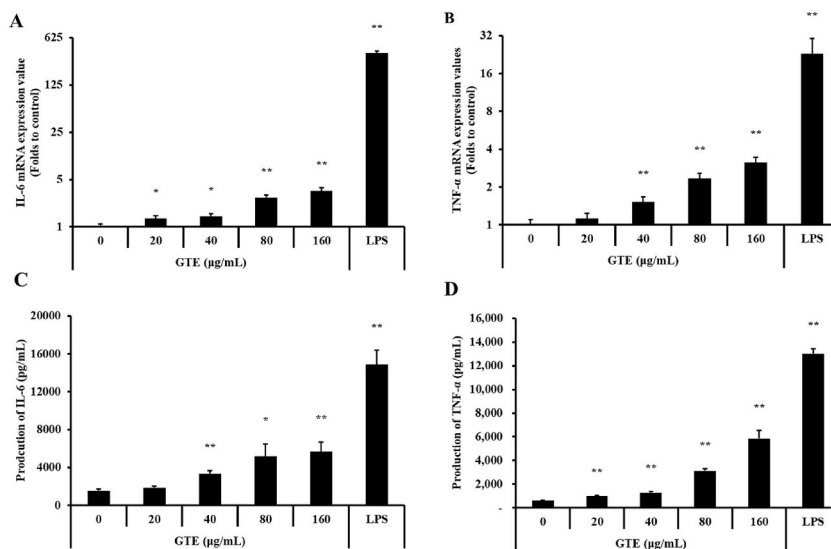


Fig. 5. Influence of green tea extract (GTE) on RAW 264.7 cell immune activity. (A) Effect of different GTE concentrations on Interleukin (IL)-6 mRNA expression, (B) tumor necrosis factor (TNF)- α , (C) IL-6 production, and (D) TNF- α production. Lipopolysaccharide (LPS) used as positive control. Mean values \pm SD (n = 3). **p < 0.01 vs. NC group.

[25–27]. In the present study, GTE improved the shape of the spleen and significantly increased its index. In addition, helper T cell (CD3⁺CD4⁺) counts significantly recovered after GTE administration, consistent with the results of the spleen histopathological analysis. According to previous studies, GTE enhances lymphoblasts to induce lymphocyte production, and EGCG, the most enriched polyphenol in green tea leaves, can modulate CD4⁺ T cell differentiation [28–30]. These findings are consistent with those of the present study. Thus, GTE can be used as a supplementary substance to induce T-cell differentiation during chemotherapy.

Macrophages play a crucial role in protecting the body via the swallowing and digestion of foreign substances and contribute to host defense mechanisms as a part of the innate immune system [31]. The cytotoxic function of macrophages in tumors depends on stimulation with bacterial cell wall components such as LPS. Stimulated macrophages secrete several substances related to tumor cell death and immune modulation, such as TNF, ROS, and NO, which can be used as indicators to evaluate the activation of RAW 264.7 cells [32–35]. Moreover, macrophages participate in the immune regulation of tumor cells through various molecular mechanisms [31].

MAPK signaling mediates cellular responses to several stimuli [36]. Activation of the MAPK pathway is caused by ROS molecules that activate the NF- κ B signaling pathway [37,38], which, in particular, induces the activation of transcription factors such as NF- κ B, thereby inducing the production of immunomodulatory factors in macrophages [39].

Here, GTE was found to effectively stimulate mouse RAW 264.7 cells and increase the production of NO, ROS, and cytokines via the MAPK signaling pathway, followed by the NF- κ B signaling pathway. According to a previous study, green tea upregulated the mRNA levels of IL-1 β , IL-6, and TNF- β in the spleen [40]. Furthermore, EGCG, the main ingredient of green tea, stimulates the production of IL-1 α , IL-1 β , monocytes, and lymphocytes [30]. These reports and results of the present study imply that GTE can stimulate the immune activity of macrophages via the activation of NF- κ B and the MAPK pathway, suggesting that GTE can be used as a clinical antitumor adjuvant.

In conclusion, using a CP-induced immunosuppressed mouse model and RAW 264.7, we showed that GTE significantly enhanced immune functions in immunosuppressed mice and activated RAW 264.7 cells via the MAPK signaling pathway. Although the current study has several limitations (first, cell experiments were not performed with primary T cells; second, GTE can be metabolized and converted into other metabolites; third, possible mechanisms of action of GTE were investigated at the cellular level only), our results indicate that GTE may act as a potential supplementary substance or clinical antitumor adjuvant during the course of chemotherapy, including that of CP.

5. Conclusion

The current study demonstrates that GTE reduces cyclophosphamide-induced immunosuppression in mice and stimulates immune activity in RAW 264.7 cells. GTE significantly improved immune function, including the spleen index and proliferation of splenic T lymphocytes. In addition, GTE effectively activated RAW 264.7, as represented by the induction of NO, ROS, and cytokine levels through the MAPK pathway. These findings suggest that GTE has the potential to be used as a supplemental agent in chemotherapy for CP.

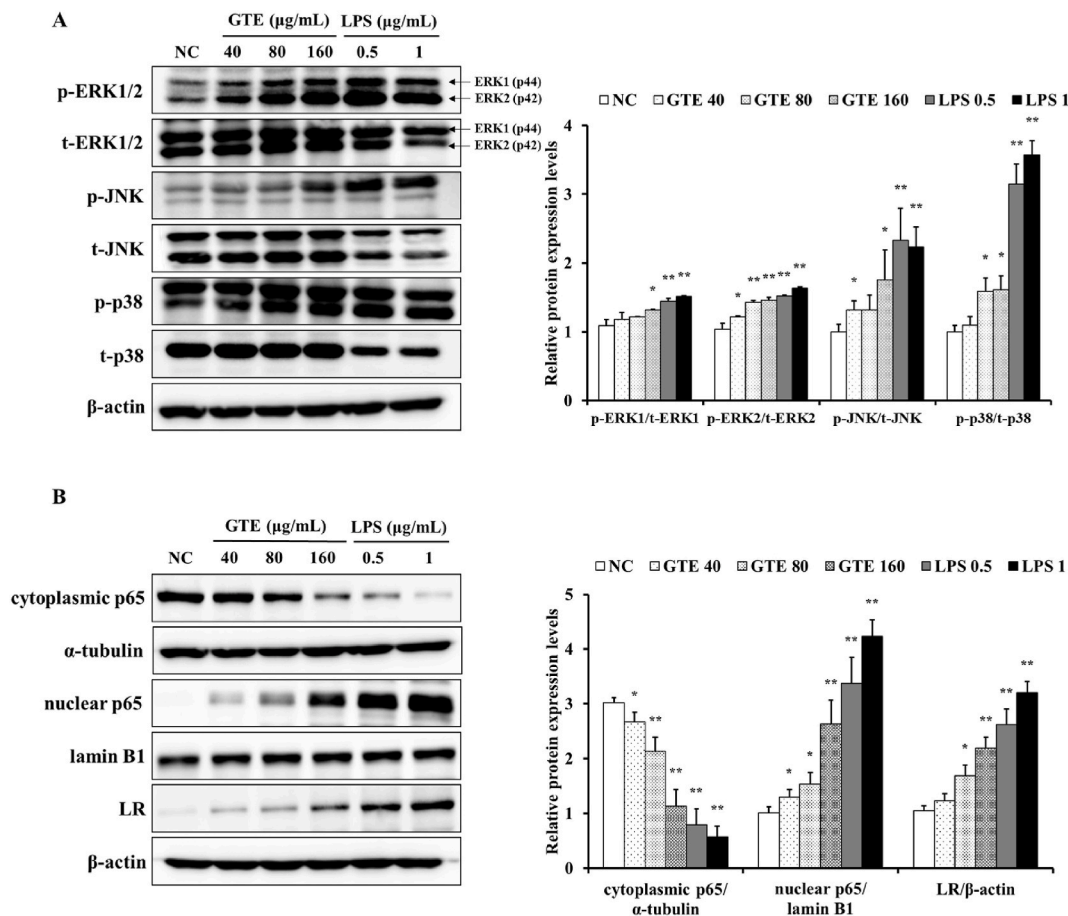


Fig. 6. Impact of green tea extract (GTE) on RAW 264.7 cell immune activity through mitogen-activated protein kinases (MAPKs) and nuclear factor kappa B (NF-κB) signaling pathways. (A) Representative band images and densitometric values of (A) MAPKs, and (B) cytoplasmic/nuclear p65 and laminin receptor (LR). Lipopolysaccharide (LPS) used as positive control. Mean values ± SD (n = 3). *, **p < 0.05 and 0.01, respectively, vs. NC group.

Funding statement

This work was supported by the research fund of Chungnam National University and Basic Science Research Program through the National Research Foundation of Korea (NRF) funded by the Ministry of Education (2021R1A6A1A03045495). This work was supported by the National Research Foundation of Korea (NRF) grant funded by the Korean government (MSIT) (2021R1A4A1033078).

Data availability statement

Data will be made available on request.

Declaration of competing interest

The authors declare that they have no known competing financial interests or personal relationships that could have appeared to influence the work reported in this paper.

References

- [1] M. Ahlmann, G. Hempel, The effect of cyclophosphamide on the immune system: implications for clinical cancer therapy, *Cancer Chemother. Pharmacol.* 78 (4) (2016) 661–671.
- [2] E. Gómez-Figueroa, E. Gutierrez-Lanz, A. Alvarado-Bolaños, et al., Cyclophosphamide treatment in active multiple sclerosis, *Neurol. Sci.* 42 (9) (2021), 3775–3780.
- [3] P. Hajdinák, M. Szabó, E. Kiss, et al., Genetic polymorphism of GSP-1 affects cyclophosphamide treatment of autoimmune diseases, *Molecules* 25 (7) (2020) 1542.

- [4] Q. Huang, L. Feng, L. Hang, et al., Jian-pi-bu-xue-formula alleviates cyclophosphamide-induced myelosuppression via up-regulating NRF2/HO1/NQO1 signaling, *Front. Pharmacol.* 11 (2020) 1302.
- [5] Y.H. Liu, H.Y. Qin, Y.Y. Zhong, et al., Neutral polysaccharide from *Panax notoginseng* enhanced cyclophosphamide antitumor efficacy in hepatoma H22-bearing mice, *BMC Cancer* 21 (1) (2021) 37.
- [6] A. Iqbal, M.K. Iqbal, S. Sharma, et al., Molecular mechanism involved in cyclophosphamide-induced cardiotoxicity: old drug with a new vision, *Life Sci.* 218 (2019) 112–131.
- [7] E. Hughes, M. Scurr, E. Campbell, et al., T-cell modulation by cyclophosphamide for tumour therapy, *Immunology* 154 (1) (2018) 62–68.
- [8] K. Dunleavy, M.A. Fanale, J. Abramson, et al., Dose-adjusted EPOCH-R (etoposide, prednisone, vincristine, cyclophosphamide, doxorubicin, and rituximab) in untreated aggressive diffuse large B-cell lymphoma with MYC rearrangement: a prospective, multicentre, single-arm phase 2 study, *Lancet Haematol* 5 (12) (2018), e609–e617.
- [9] C.P. Venner, R. LeBlanc, I. Sandhu, et al., Weekly carfilzomib plus cyclophosphamide and dexamethasone in the treatment of relapsed/refractory multiple myeloma: final results from the MCRN-003/MYX.1 single arm phase II trial, *Am. J. Hematol.* 96 (5) (2021) 552–560.
- [10] M.I. Prasanth, B.S. Sivbamaruthi, C. Chaiyasut, et al., A review of the role of green tea (*Camellia sinensis*) in anti-photoaging, stress resistance, neuroprotection, and autophagy, *Nutrients* 11 (2) (2019) 474.
- [11] J.W. Kim, C.Y. Kim, J.H. Kim, et al., Prophylactic catechin-rich green tea extract treatment ameliorates pathogenic enterotoxigenic *Escherichia coli*-induced colitis, *Pathogens* 10 (12) (2021) 1573.
- [12] G.Y. Tang, X. Meng, R.Y. Gan, et al., Health functions and related molecular mechanisms of tea components: an update review, *Intermt. J. Sci.* 20 (24) (2019) 6196.
- [13] S.A. Almatroodi, A. Almatroodi, A.A. Khan, et al., Potential therapeutic targets of epigallocatechin gallate (EGCG), the most abundant catechin in green tea, and its role in the therapy of various types of cancer, *Molecules* 25 (14) (2020) 3146.
- [14] S. Wang, Z. Li, Y. Ma, et al., Immunomodulatory effects of green tea polyphenols, *Molecules* 26 (12) (2021) 3755.
- [15] M. Hong, L. Cheng, Y. Liu, et al., A natural plant source-tea polyphenols, a potential drug for improving immunity and combating virus, *Nutrients* 14 (3) (2022) 550.
- [16] J. Schwager, N. Seifert, A. Bompard, et al., Resveratrol, EGCG and vitamins modulate activated T lymphocytes, *Molecules* 26 (18) (2021) 5600.
- [17] M. Pae, D. Wu, Immunomodulating effects of epigallocatechin-3-gallate from green tea: mechanisms and applications, *Food Funct.* 4 (9) (2013) 1287–1303.
- [18] Y. Singh, M.S. Salker, F. Lang, Green tea polyphenol-sensitive calcium signaling in immune T cell function, *Front. Nutr.* 7 (2021), 616934.
- [19] J.W. Ko, N.R. Shin, J.O. Lim, et al., Silica dioxide nanoparticles aggravate airway inflammation in an asthmatic mouse model via NLRP3 inflammasome activation, *Regul. Toxicol. Pharmacol.* 112 (2020), 104618.
- [20] I.S. Shin, M.Y. Lee, H. Ha, et al., *Dianthus superbus fructus* suppresses airway inflammation by downregulating of inducible nitric oxide synthase in an ovalbumin-induced murine model of asthma, *J. Inflamm.* 9 (1) (2012) 41.
- [21] T. Kitamura, B.Z. Qian, J.W. Pollard, Immune cell promotion of metastasis, *Nat. Rev. Immunol.* 15 (2) (2015) 73–86.
- [22] M.H. Centella, A.G. Alejandra, P.S. Roberto, et al., Marine-derived bioactive compounds for value-added applications in bio- and non-bio sectors, *J. Clean. Prod.* 168 (2017) 1559–1565.
- [23] L. Zitvogel, L. Apetoh, F. Ghiringhelli, et al., Immunological aspects of cancer chemotherapy, *Nat. Rev. Immunol.* 8 (1) (2008) 59–73.
- [24] J. Saravia, N.M. Chapman, H. Chi, Helper T cell differentiation, *Cell. Mol. Immunol.* 16 (7) (2019) 634–643.
- [25] M. Miao, B. Cheng, L. Guo, et al., Effects of Fuzheng Paidu tablet on peripheral blood T lymphocytes, intestinal mucosa T lymphocytes, and immune organs in cyclophosphamide-induced immunosuppressed mice, *Hum. Vaccines Immunother.* 11 (11) (2015) 2659–2663.
- [26] K. Hagihara, T. Yamane, Y. Aoyama, et al., Evaluation of an automated hematology analyzer (CELL-DYN 4000) for counting CD4+ T helper cells at low concentrations, *Ann Clin Sci* 35 (1) (2005) 31–36.
- [27] X. Zhou, Q. Dong, X. Kan, et al., Immunomodulatory activity of a novel polysaccharide from *Lonicera japonica* in immunosuppressed mice induced by cyclophosphamide, *PLoS One* 13 (10) (2018), e0204152.
- [28] Y. Zhou, X. Chen, R. Yi, et al., Immunomodulatory effect of tremella polysaccharides against cyclophosphamide-induced immunosuppression in mice, *Molecules* 23 (2) (2018) 239.
- [29] D. Ravindran Menon, Y. Li, T. Yamauchi, et al., EGCG inhibits tumor growth in melanoma by targeting JAK-STAT signaling and its downstream PD-L1/PD-L2-PD1 Axis in tumors and enhancing cytotoxic T-cell responses, *Pharmaceuticals* 14 (11) (2021) 1081.
- [30] D. Wu, J. Wang, M. Pae, et al., Green tea EGCG, T cells, and T cell-mediated autoimmune diseases, *Mol. Aspect. Med.* 33 (1) (2012) 107–118.
- [31] J. Zhou, Z. Tang, S. Gao, et al., Tumor-Associated macrophages: recent insights and therapies, *Front. Oncol.* 10 (2020) 188.
- [32] A.H. Klimp, E.G. de Vries, G.L. Scherphof, et al., A potential role of macrophage activation in the treatment of cancer, *Crit. Rev. Oncol. Hematol.* 44 (2) (2002) 143–161.
- [33] Y. Zhang, S. Choksi, K. Chen, et al., ROS play a critical role in the differentiation of alternatively activated macrophages and the occurrence of tumor-associated macrophages, *Cell Res.* 23 (7) (2013) 898–914.
- [34] A. Ramesh, S. Kumar, A. Brouillard, et al., A nitric oxide (NO) nanoreporter for noninvasive real-time imaging of macrophage immunotherapy, *Adv. Mater.* 32 (24) (2020), e2000648.
- [35] E.B. Kopp, S. Ghosh, NF-kappa B and rel proteins in innate immunity, *Adv. Immunol.* 58 (1995) 1–27.
- [36] E.K. Choi, J.S. Yeo, C.Y. Park, et al., Inhibition of reactive oxygen species downregulates the MAPK pathway in rat spinal cord after limb ischemia reperfusion injury, *Int. J. Surg.* 22 (2015) 74–78.
- [37] S.K. Jalmi, A.K. Sinha, ROS mediated MAPK signaling in abiotic and biotic stress- striking similarities and differences, *Front. Plant Sci.* 6 (2015) 769.
- [38] Y. Son, Y.K. Cheong, N.H. Kim, et al., Mitogen-activated protein kinases and reactive oxygen species: how can ROS activate MAPK pathways? *J Signal Transduct* 2011 (2011), 792639.
- [39] N. Wang, H. Liang, K. Zen, Molecular mechanisms that influence the macrophage m1-m2 polarization balance, *Front. Immunol.* 5 (2014) 614.
- [40] S. Nootash, N. Sheikhzadeh, B. Baradaran, et al., Green tea (*Camellia sinensis*) administration induces expression of immune relevant genes and biochemical parameters in rainbow trout (*Oncorhynchus mykiss*), *Fish Shellfish Immunol.* 35 (6) (2013) 1916–1923.